Anchoring of Copper(II) Acetylacetonate onto an Activated Carbon Functionalised with a Triamine

Ana Rosa Silva,[a] Magda Martins,[a] M. Madalena A. Freitas,[b,c] José Luís Figueiredo,[b] Cristina Freire,*[a] and Baltazar de Castro[a]

Keywords: Copper / Schiff bases / Activated carbon / Anchoring / EPR spectroscopy

Copper(II) acetylacetonate was anchored onto a triamine functionalised activated carbon by Schiff condensation using a four-step procedure: (i) oxidation of activated carbon with nitric acid; (ii) treatment with thionyl chloride to convert carbon surface carboxylic acids into acyl chlorides; (iii) condensation of acyl chloride functionalities with amine groups of bis(3-aminopropyl)amine (*trien*); and (iv) Schiff condensation between free amine groups of bound *trien* with the oxygen atoms of acetylacetonate coordinated to the copper(II) ion. The same complex was also anchored to the unmodified activated carbon and to the acyl chloride functionalised carbon prepared in (ii). The resulting carbon-based materials were characterised by elemental analysis, surface techniques (SEM and XPS), temperature programmed desorption, and nitrogen adsorption at 77 K and EPR spectroscopy for the materials with copper(II) complexes. Data from all techniques provided evidence for (i) the covalent binding of *trien* to acyl chloride functionalities; and (ii) the irreversible attachment of $[Cu(acac)_2]$ to all carbon-based materials. Data for the materials with copper(II) proved conclusively that only the immobilisation procedure based on Schiff condensation with *trien* led to copper(II) complexes in which the metal centre remains four-coordinate.

Introduction

Aziridines are very important intermediates in organic synthesis and copper(II) acetylacetonate has been described as a very efficient homogeneous catalyst for the aziridination of olefins.[1] Copper(II) Schiff-base complexes have also been used as homogeneous catalysts in the aziridination of olefins,[2] as well as in the cyclopropanation of olefins,[3] oxidation of sulfides to sulfoxides[4] and in the peroxidative oxidation of phenol to dihydroxy benzynes.[5] Currently, transition metal complexes with Schiff-base ligands (*salen*) are the subject of intense research as they present high activity, chemoselectivity and enantioselectivity in a large range of catalytic processes.[6]

The last decade has witnessed a growing interest in the heterogenisation of homogeneous metal complexes using several types of supports,[6−10] with the aim to overcome some limitations of homogeneous catalysts − separation from the reaction media and subsequent recycling. Initially the complexes were ion exchanged or adsorbed on the porous supports and, consequently, could be susceptible to leaching.[10−12] More recently, several grafting and tethering procedures have been developed to covalently attach transition metal complexes to organic polymers,[8] silica, zeolites and other micro and mesoporous inorganic materials.[7,9,10]

Activated carbons and other carbon materials are widely used as catalysts and as supports for metals in its reduced state,[13,14] and few reports have appeared in the last years on the heterogenisation of homogeneous metal complexes, mainly of noble metals with simple ligands, to be used in hydrogenation and hydroformylation reactions.[15−17] Nevertheless, activated carbons present several advantages when compared to inorganic supports;[13] they are thermally stable, resistant to chemical attack in acid and basic media and, generally, of low cost.[13] On the other hand, several thermal and chemical processes can be used to tailor the porous structure and the type and concentration of specific oxygen surface groups.[13,18] These groups can be used as building blocks to bridge the metal complex to the support, and their variety allows for the use of various immobilisation procedures. Iron−phthalocyanine complexes supported by impregnation on carbon[19] and activated carbon blacks[20] have been used as heterogeneous catalysts in the oxidation of alkanes, but no reference to leaching or

[a] REQUIMTE/Departamento de Química, Faculdade de Ciências, Universidade do Porto,
4169-007 Porto, Portugal
Fax: (internat.) + 351-22-6082959
E-mail: acfreire@fc.up.pt
[b] Laboratório de Catálise e Materiais, Departamento de Engenharia Química, Faculdade de Engenharia, Universidade do Porto,
4200-465 Porto, Portugal
[c] Instituto Superior de Engenharia, Instituto Politécnico do Porto,
4200-072 Porto, Portugal

reuse was made, despite the method used being susceptible to leaching of the active phase. Anchorage of copper(II) and cobalt(II) acetylacetonates to surface groups of an activated carbon using a diamine as linking agent has also been reported, and resulting materials have not only proved to be efficient heterogeneous catalysts in the oxidation of pinane, but were also resistant to leaching of the complexes.[21]

We are pursuing the development of several strategies for the immobilisation of functionalised Schiff-base transition metal complexes onto activated carbons in order to gather information on whether the modifications of their surface groups can lead to a more efficient anchoring without loss of catalytic activity of the complex, with the overall aim of optimising procedures to prepare carbon-based heterogeneous catalysts. Recently, we have reported the anchoring of nickel(II) Schiff-base complexes onto activated carbon using two different routes;[22,23] in the first a linking agent, cyanuric chloride, was used to react with hydroxyl groups on both the activated surface and the metal complex;[22] and in the second, two metal complexes bearing uncoordinated amine groups were anchored onto an activated carbon functionalised with an acyl chloride that acted as the anchoring building block functionality.[23] The direct anchoring of a copper(II) Schiff-base complex functionalised with uncoordinated hydroxyl groups was achieved[24] and the process was applied to the heterogenisation of their manganese(III) counterparts, which were shown to act as efficient and reusable heterogeneous catalysts in the epoxidation of styrene,[25,26] with similar styrene epoxide chemoselectivities as the corresponding homogeneous phase reactions.[25,26,27]

Copper(II) complexes with pentadentate N_3O_2 Schiff bases have also been encapsulated in zeolites[28,29] and in aluminium pillared layered clays using the ship in a bottle procedure,[30,31] by reaction of copper(II) acetylacetonate with bis(3-aminopropyl)amine (*trien*), and using the simultaneous pillaring and copper(II) complex encapsulation in a montmorilonite.[32] In the present work, we report an extension of these procedures in which copper(II) acetylacetonate is irreversibly anchored onto a chemically oxidised activated carbon functionalised with *trien* by Schiff condensation between the free amine groups of *trien* covalently attached to the activated carbon surface (see Scheme 1) with the oxygen atoms of acetylacetonate coordinate to copper(II) (see Scheme 2). To assess the effectiveness of this method we have compared its anchoring efficiency with those obtained by direct adsorption onto unmodified oxidised activated carbon and onto a carbon functionalised with acyl chloride groups. In order to get information on the effect of the various treatments on the surface chemical and physical properties of the carbon materials, these were characterised by proximate and elemental analysis, surface techniques (scanning electron microscopy and X-ray photoelectron spectroscopy), nitrogen adsorption at 77 K, and thermal methods (temperature-programmed desorption). Copper(II) carbon-based materials were also characterised by electron paramagnetic resonance, which can provide information on the changes in the coordination sphere of the metal centre.

Results and Discussion

Immobilisation of copper(II) acetylacetonate onto the activated carbon was performed in four steps: (i) oxidation of the activated carbon with nitric acid, (ii) reaction with $SOCl_2$, (iii) functionalisation with *trien*, bis(3-aminopropyl)-amine, and then (iv) anchoring of the complex onto the modified carbon. The materials obtained after the first two steps of the anchoring procedure (carbon A2 and A3) have been extensively characterised by us in a previous report,[23] and thus the characterisation and discussion will be focused on the new materials obtained from the two last steps.

Functionalisation of Thionyl-Chloride-Modified Activated Carbon with Bis(3-aminopropyl)amine (*trien*)

Composition and Texture

The proximate and elemental analyses of carbon materials are collected in Table 1. The volatile matter and the nitrogen and hydrogen content increase when carbon A3 is modified with *trien* (Table 1), suggesting that *trien* reacted with the activated carbon surface groups and therefore was covalently attached to the activated carbon surface. This is also supported by a decrease, relative to carbon A3, of 16% in the micropore volume and of 19% in the larger pore area (Table 2), arising from the presence of a relatively voluminous compound at the surface of the activated carbon.

Table 1. Proximate and elemental analyses for carbon-based materials.

Carbon atom	Proximate analysis (wt.-%) volatiles	C_{fixed}	ash	Elemental analysis (wt.-%) C	H	N
A1	8.81	89.44	1.74	92.69	0.44	0.45
A2	11.78	87.28	0.95	91.04	0.36	0.73
A3	21.11	78.37	0.52	89.31	1.12	0.51
A4	23.78	76.19	0.03	88.57	1.49	1.20
A5	19.29	79.51	1.20	87.57	1.08	1.17

Table 2. Textural properties for carbon-based materials

Carbon	V_{micro}[a] ($cm^3\ g^{-1}$)	S_{me}[a] ($m^2\ g^{-1}$)	$V_{0.95}$[b] ($cm^3\ g^{-1}$)	V_{meso}[c] ($cm^3\ g^{-1}$)
A1	0.359	122	0.527	0.168
A2	0.347	122	0.516	0.169
A3	0.303	255	0.581	0.278
A4	0.255	207	0.514	0.259
A5	0.222	74	0.330	0.107

[a] Calculated by the *t*-method. [b] Pore volume at $p/p_0 = 0.95$. [c] Subtraction of the total pore volume, at $p/p_0 = 0.95$, and of the microporous volume.

X-ray Photoelectron Spectroscopy

There is a significant increase in the nitrogen content following the introduction of *trien* in carbon A3, which is accompanied by a decrease in the chlorine content as can be seen in Table 3. This indicates that reaction between the amine groups of the triamine and the acyl chloride functionalities has occurred, with formation of new amide groups and loss of hydrogen chloride (Scheme 1, a). A superficial loss of oxygen is also observed which may be explained by Schiff condensation between the amine groups and the surface carbonyl groups (Scheme 1, b, see TPD section, below), that increases the effectiveness of the *trien* anchoring process.

Table 3. Area under the XPS bands in the O 1s, N 1s, Cl 2p, C 1s, and Cu $2p_{3/2}$ regions of the carbon-based materials

Carbon atom	Atomic % O	N	Cl	C	Cu	O/C	N/C	Cl/C	N/Cu
A1	7.66	0.58	0.86	90.41	–	0.0847	0.0064	0.0095	–
A2	20.27	0.58	0.13	78.61	–	0.2578	0.0074	0.0017	–
A3	10.98	0.60	3.03	84.84	–	0.1294	0.0071	0.0357	–
A4	9.01	3.64	1.81	85.06	–	0.106	0.0428	0.0213	–
A5	14.01	4.48	2.20	78.16	0.66	0.1792	0.0573	0.0281	6.8

The Cl 2p spectrum of carbon A4 exhibits bands at the same binding energy as those found in the parent material (Figure 1, a), thus providing evidence that not all surface acyl chloride functionalities have reacted with the amine groups of *trien*. A new band is also observed at about 199 eV, which corresponds to chloride ions produced in the reaction of acyl chloride with amine groups (Scheme 1, a).

The spectra of carbons A3 and A4 in the O 1s region are similar (Figure 1, b), but that of carbon A4 shows a very slight band broadening, which may suggest an increase in the amount of oxygen atoms in different chemical environments resulting from the new amide ligation (Scheme 1, a).

The XPS spectrum of carbon A4 in the N 1s region (Figure 1, c) presents an almost symmetrical large band, centred at about 400 eV, which corresponds to different types of nitrogen atoms present at the surface of the carbon material – primary amines, secondary amines, amides and imines (Scheme 1).[33]

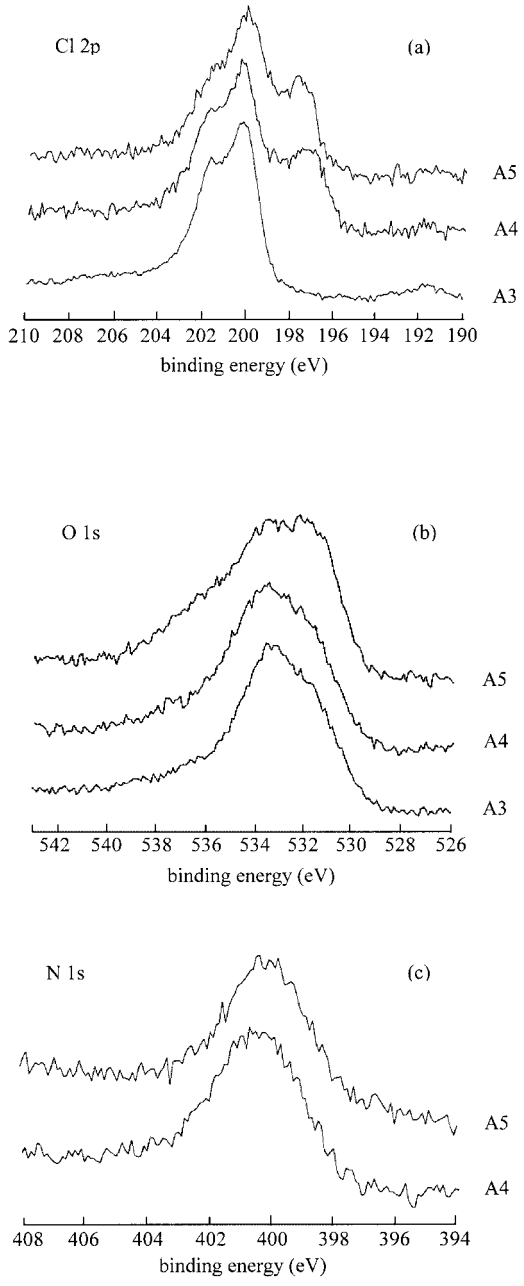

Figure 1. High resolution XPS spectra of carbon-based materials in the regions: a) Cl 2p; b) O 1s, and c) N 1s

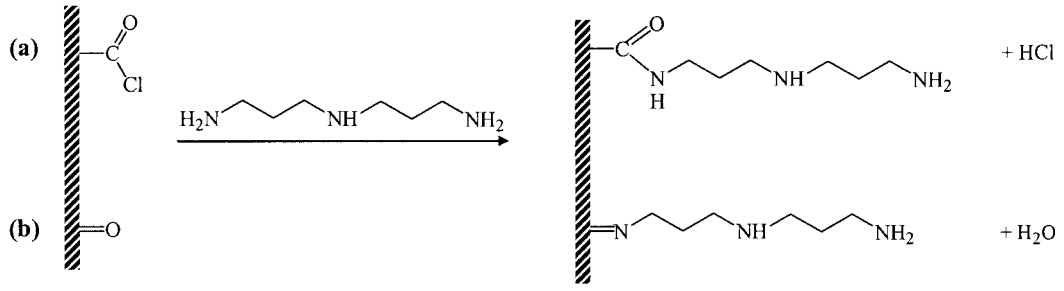

Scheme 1. Anchoring of *trien* onto acyl chloride functionalised activated carbon

Temperature Programmed Desorption (TPD)

The TPD profiles for the $m/z = 28$ and $m/z = 44$ fragments of carbon atoms A3−A5 are represented in Figure 2, and the areas under the peaks for all carbon-based materials are collected in Table 4. We have already described in a previous report[23] that oxidation of activated carbons with nitric acid increases the number of carboxylic acid groups which are observed at 560 K in the $m/z = 44$ TPD profile.

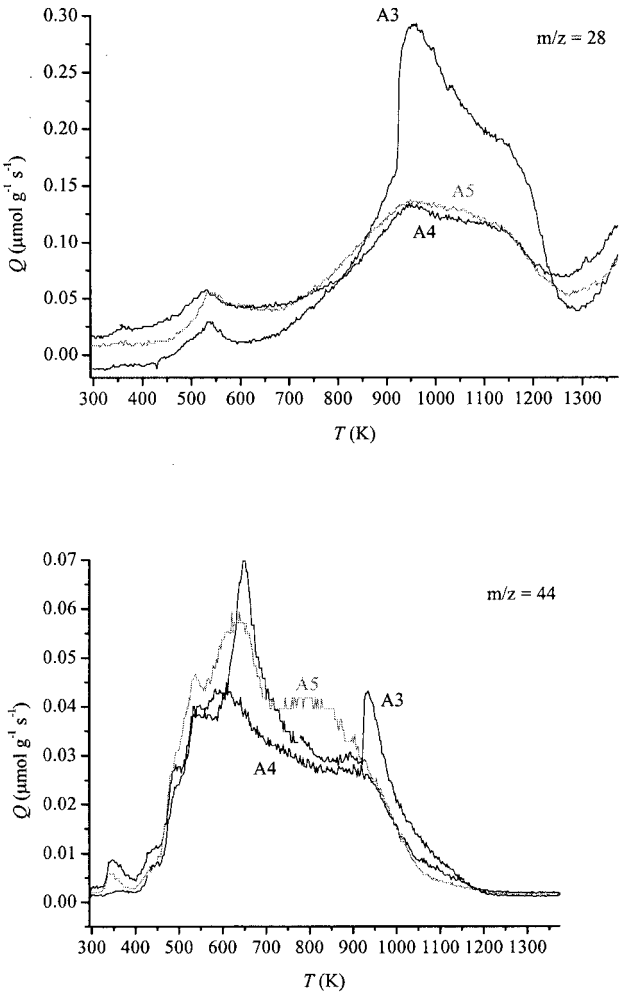

Figure 2. TPD profiles for the fragments $m/z = 28$ and 44 for A3−A5 carbon-based materials

Table 4. Amounts of fragments with $m/z = 28$ and $m/z = 44$ released during the TPD experiments, obtained by integration of the areas under the peaks, for the carbon-based materials

Carbon atom	$m/z = 28$ (μmol g^{-1})	$m/z = 44$ (μmol g^{-1})	$m/z = 28 + 44$ (μmol g^{-1})
A1	476	140	616
A2	1046	374	1420
A3	1270	245	1515
A4	712	201	913
A5	787	254	1041
A6	1041	314	1355
A7	1014	259	1273

These bands disappear after reaction with thionyl chloride, giving rise to a new intense band at 960 K in the $m/z = 28$ TPD profile, which has been attributed to the acyl chloride functionalities.[23] These functionalities decompose to carbon monoxide, but at lower temperature than the carbonyl/quinone functionalities (1100 K) due to the electron density withdrawing effect of chlorine atom. Introduction of the triamine at the surface of carbon A3 causes a significant decrease in intensity of the band at 960 K in the $m/z = 28$ TPD profile (Figure 2). This phenomenon was also observed upon the attachment of nickel(II) complexes functionalised with amines onto an activated carbon surface with acyl chloride functionalities and was attributed to the reaction between the amine groups and the acyl chloride groups, with the formation of amide ligations.[23] The same explanation is presupposed for the decrease in intensity of this band after the reaction of amine groups of *trien* with acyl chloride surface groups (Scheme 1, a).

There is also a significant intensity decrease in the high temperature region of the $m/z = 28$ TPD profile (Figure 2, b) assigned to carbonyl groups, which may be attributed to Schiff condensation reactions between these groups and the amines (Scheme 1, b), in accordance with the results of XPS analysis (vide supra).

Anchoring of the Copper(II) Acetylacetonate onto the Modified Activated Carbons

Evidence for the effective anchorage of the copper complexes onto the surface of carbon A4 is provided by noting that (a) the blue colour of complex solution disappears during the adsorption reaction, and (b) colourless solutions are obtained when the material is purified by Soxhlet extraction.

Adsorption of copper(II) acetylacetonate (toluene solutions) onto carbons A2 and A3 was also performed using similar experimental conditions and a decrease in the blue colour of solution was observed. During the purification steps of these materials no colour due to copper(II) complexes were observed in the washing solutions, suggesting that the adsorbed copper(II) acetylacetonate was not leached.

Copper content of carbons A5−A7 was determined by ICP-AES and from this it was possible to calculate the loading (mass of copper/mass of carbon × 100) and the efficiency of adsorption (amount of adsorbed complex/amount in original solution × 100) which are both summarised in Table 5. The data shows that metal loading in A6 and A7 are similar, but are about half of that in A5, with a similar pattern for the efficiency of adsorption. These results clearly indicate that functionalisation of the activated carbon surface with a triamine increases the efficiency of copper(II) acetylacetonate immobilisation.

Composition and Texture

A comparison of the results of proximate and elemental analyses of carbon A5 with those of its precursor (carbon

Table 5. ICP-AES results for copper containing carbon-based materials

Carbon atom	n_i[a] (μmol g^{-1})	Cu (wt-%)	n_f[b] (μmol g^{-1})	η[c] (%)	N/Cu[d]
A5	145	0.779 (3.12)[e]	123	85	6.8
A6	168	0.396	62	37	–
A7	114	0.382	60	53	–

[a] n_i = initial $[Cu(acac)_2]$ mol (solution)/weight activated carbon. [b] n_f = adsorbed $[Cu(acac)_2]$ moles/weight activated carbon. [c] $\eta = n_f \times 100/n_i$. [d] N/Cu (atomic ratio) =[N(wt%) × relative atomic mass(Cu)]/[Cu(wt%) × relative atomic mass(N)]; N(wt%) from Table 1. [e] Copper weight% calculated from XPS in Table 3. Weight Cu% = atomic% Cu × Ar(Cu)/[atomic% O × Ar(O) + atomic% N × Ar(N) + atomic% Cl × Ar(Cl) + atomic% C × Ar(C) + atomic% Cu × Ar(Cu)].

A4) show an increase in ash content, and a decrease in hydrogen content. The first is due to the presence of copper(II) in the material, and the second further supports the immobilisation of $[Cu(acac)_2]$ by the processes represented in Scheme 2, due to loss of water during Schiff condensation.

The decrease of volatile matter after complex anchorage may be attributed to the inclusion of *trien* in the copper(II) coordination sphere (Scheme 2), which increases its stability relative to that of *trien* bound only to the activated carbon surface.

The immobilisation of copper(II) acetylacetonate onto carbon A4 causes pore blockage and thus a decrease in pore volume. The observation that the decrease (59%) in wide pore volume is much larger than that observed (13%) in micropore volume suggests that the metal complexes are anchored preferentially onto the mesopore and macropore surface.

X-ray Photoelectron Spectroscopy

High resolution XPS spectra of carbons A3−A5 in the O 1s region are depicted in Figure 1, and the areas under the high resolution XPS peaks in the regions O 1s, N 1s, Cl 2p, C 1s, and Cu $2p_{3/2}$ are summarised in Table 3.

When $[Cu(acac)_2]$ is immobilised onto the activated carbon functionalised with *trien* there is an increase in oxygen and copper surface content (Table 3), but no significant changes are observed in the XPS spectra, with the exception of the O 1s XPS profile, for which an increase in intensity of the lower energy band (531.6 eV) is observed (Figure 1). Since we reported that oxygen atoms coordinated to transition metal cations possess similar O 1s binding energies,[22−26] this increase may be assigned to oxygen atoms from $[Cu(acac)_2]$.

By using the Cu atomic% from XPS and converting to Cu wt% we get 3.12 (Table 5), a value that when compared with Cu wt% from bulk analysis (0.779), indicates that the complexes are located preferentially at the outer pores.

An atomic ratio N/Cu of 6.8 is obtained by both XPS (Table 3) and elemental analysis (Table 5), which provides an indication that the anchoring mechanism of $[Cu(acac)_2]$ is the same within the matrix. The atomic ratio N/Cu for anchored complexes must lie between 3 and 6 (Scheme 2), thus the observed value is consistent with the presence of uncomplexed *trien*, but does not provide any conclusive information on *trien* binding to copper.

Temperature Programmed Desorption

Carbons A4 and A5 exhibit TPD profiles that are practically identical for $m/z = 28$ and slightly different for $m/z = 44$ (Figure 2), which suggests that the main anchoring process takes place by reaction with the amine groups immobilised at the carbon A4 surface, and that direct complex anchoring to the oxygen groups on the carbon surface must be virtually absent. The small differences in the $m/z = 44$ profile between A5 and A4 carbons may be assigned to fragments arising from decomposition of acetylacetonate ligand.

This result must be contrasted with the changes in the TPD profiles of carbon atoms A6 and A7, which exhibit a decrease in band intensity when compared with those of their precursors (A2 and A3) (Figures 3 and 4, respectively). For A6, those corresponding to carbonyl/quinone groups

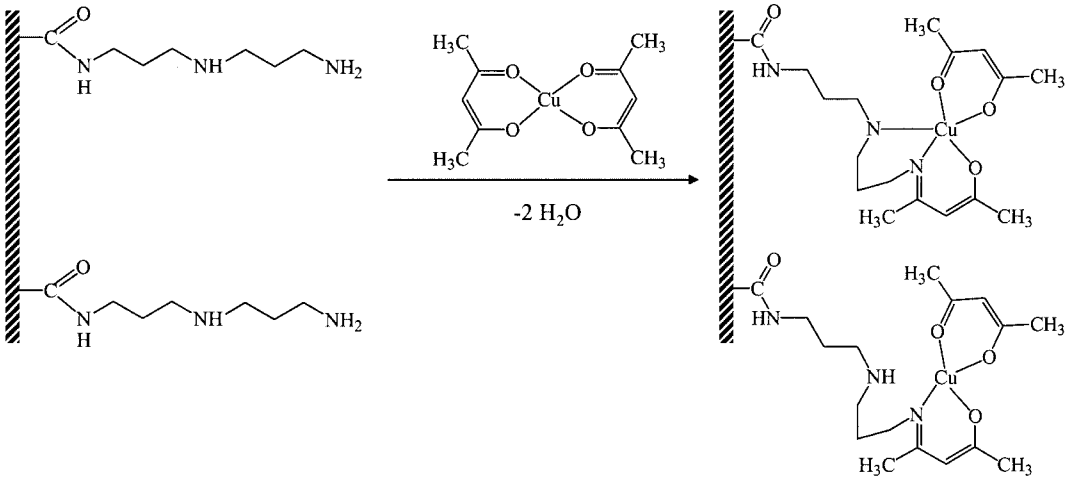

Scheme 2. Proposed structures for the anchored copper(II) acetylacetonate onto *trien* functionalised activated carbon

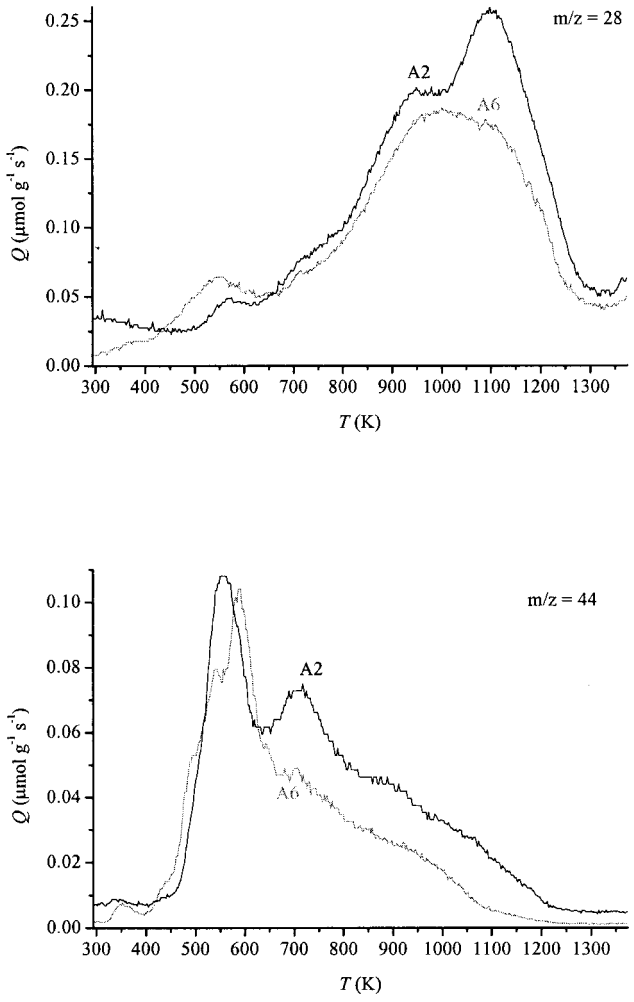

Figure 3. TPD profiles for the fragments m/z = 28 and 44 for A2 and A6 carbon-based materials

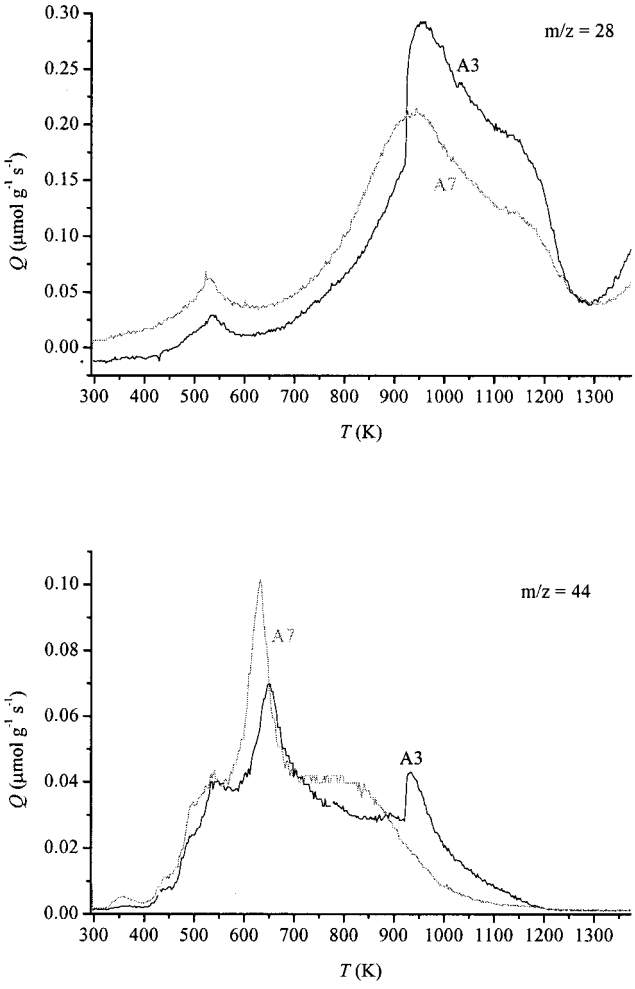

Figure 4. TPD profiles for the fragments m/z = 28 and 44 for A3 and A7 carbon-based materials

(higher temperatures in the m/z = 28 profile)[18] and to lactones and anhydrides (m/z = 44 profile).[18] A similar pattern is also observed for A7, but the most characteristic feature is the decrease in the band which was assigned to acyl chloride functionalities.[23] These changes suggest direct anchoring [Cu(acac)$_2$] to surface functional groups of the activated carbons and we propose that it takes place by axial coordination of the copper(II) complex to these surface groups.

Electronic Paramagnetic Resonance

Carbon A5 exhibits an EPR spectrum of axial type which shows hyperfine splitting in the lowest magnetic field region, due to the interaction of the unpaired electron with the copper nucleus (^{65}Cu/^{63}Cu I = 3/2) (Figure 5, a). The EPR spectrum is typical of magnetically diluted copper(II) species, despite the large band broadening, which indicates that [Cu(acac)$_2$] is regularly distributed within the carbon matrix, which acts as a diamagnetic host.

The similarity between the EPR spectrum of carbon A5 with those observed for free [Cu(acac)$_2$] (Figure 5, b) and [Cu(acac)$_2$*trien*] (Figure 5, c) complexes allows the same

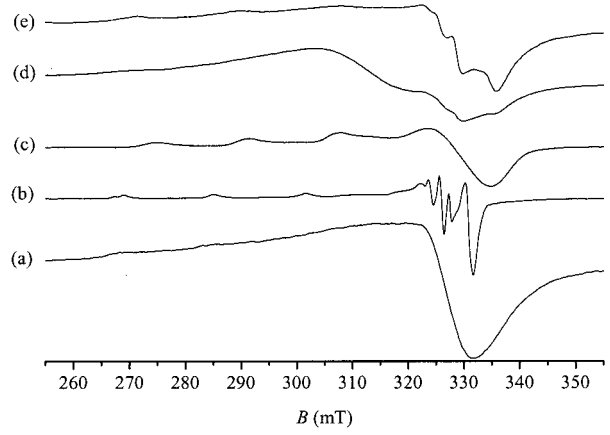

Figure 5. EPR spectra (ν = 9.41 GHz) at 120 K for: (a) carbon A5, 1% in KBr; (b) [Cu(acac)$_2$], frozen methanol solution; (c) [Cu(acac)$_2$-*trien*], frozen methanol solution; (d) A7, 5% in KBr, and (e) carbon A6, 5% in KBr

orientation scheme for the tensor axes: $g_1 = g_z$, $g_2 = g_x$, $g_3 = g_y$, where g_1 and g_3 refer to the lowest and highest magnetic fields g values (obviously, $A_1 = A_z$, $A_2 = A_x$, and $A_3 = A_y$);[34,35] in this context, as $g_z > g_x$, g_y, the ground

Table 6. EPR data for the free and supported $[Cu(acac)_2]$ complex

Sample	g or g_z	$g_\perp$ or g_x; g_y	g_{av}[a]	A[b] or A_z	$A_\perp$[b] or A_x; A_y	Ref.
$[Cu(acac)_2]/CHCl_3$	2.285	2.042	2.123	175	28.2	[34]
$[Cu(acac)_2]$/dmf	2.293	2.061	2.138	172	13.1	[34]
$[Cu(acac)_2]$/methanol	2.290	2.067	2.141	165.0	15.4	[29]
$[Cu(acac)_2$*trien*]/methanol	2.243	2.050	2.144	174.9	12.0	[29]
A5	2.288	2.063	2.138	165.7	25.7;25.7	[c]
A6	2.251	2.044; 2.050	2.115	178.7	25.7;25.7	[c]
A7	[d]	[d]	[d]	[d]	[d]	[c]

[a] $gav = 1/3(g + 2\,g_\perp)$ or $g_{av} = 1/3(gz + gx + gy)$. [b] The values are expressed in 10^{-4} cm^{-1}. [c] This work. [d] Not simulated.

state proposed for $[Cu(acac)_2]$ anchored onto activated carbon functionalised with *trien* is d_{xy}.[35]

The values of tensors g and A obtained by simulation are compiled in Table 6, as well as the values for similar copper(II) free complexes. It must be pointed out that band broadening can be attributed not only to solid state effects, but also to the presence of distinct copper(II) species with very similar structures, a consequence of the different copper coordination spheres that arise from the anchorage (Scheme 2). The existence of several species for which the g and A values are very similar makes it impossible to resolve individual spectra and the EPR simulated values must be taken as average values. Nevertheless, a careful comparison with g an A values for free copper(II) complexes can provide insights into the possible structures of the anchored complexes.

The g value of carbon atom A5 is similar to those of $[Cu(acac)_2]$ in several solvents where axial coordination is incipient or nonexistent (Table 6), suggesting that the majority of *trien* based anchored complexes are four-coordinate (probably with some tetrahedral distortion) and with no axial coordination to the nitrogen of the secondary amine of *trien* (Scheme 2). However, direct anchoring of $[Cu(acac)_2]$ by axial coordination to carbon surface groups cannot be ruled out on the basis of the EPR data, as axial coordination and tetrahedral distortion of the equatorial plane may cause similar changes in the EPR spectra.[36,37]

The EPR spectrum of carbon atom A7 (Figure 5, d) is more complex, and as it can be interpreted assuming the existence of an octahedral species (strong axial coordination to carbon surface groups), either with pseudo isotropic EPR signals or low intensity magnetic interactions between vicinal copper(II) centres, its full interpretation was not further pursued.

In contrast, the EPR spectrum of carbon atom A6 (Figure 5, e) is similar to that of A5, thus also typical of magnetically diluted species, and for which the same orientation scheme for the g and A tensor can be used, and a d_{xy} ground state proposed. However, as the g value is similar to that of $[Cu(acac)_2$*trien*] (Table 6), axial coordination of the copper(II) atom to the carbon surface groups is proposed.

Conclusion

Direct anchoring of copper(II) acetylacetonate onto an oxidised activated carbon can be achieved using either the unmodified or an acyl chloride functionalised form (Scheme 1), but in either case direct coordination of the copper(II) centres to carbon surface groups takes place. The copper(II) complex can also be immobilised in activated carbons functionalised with acyl chlorides to which bis(3-aminopropyl)amine have been immobilised, thus making the available amine groups distant from the carbon surface, which are able to covalently attach $[Cu(acac)_2]$ by amide ligations, formed by Schiff condensation of the unbound amines with the oxygen atoms of the acetylacetonate ligands.

In all methods the complexes are bound to the carbon surface and thus leaching of complexes is prevented, but the anchoring method that uses *trien* has two significant advantages. On the one hand it allows for the loading of the copper(II) complex to be larger than the other methods by a factor of two, and more importantly the separation of the copper centres from the carbon surface which implies that the majority of the anchored complexes remain four-coordinate. This latter aspect is of crucial importance if these heterogeneous materials, with anchored copper(II) complexes, are to be used to catalyse reactions for which $[Cu(acac)_2]$ acts as a homogeneous catalyst. This means that the tethered complexes retain the same coordination sphere as that in solution, making these materials very promising heterogeneous catalysts for the aziridination of olefins.

Experimental Section

Materials: The starting carbon material was a NORIT ROX 0.8 activated carbon (rodlike pellets with 0.8 mm diameter and 5 mm length). This material has a pore volume of 0.695 $cm^3 \cdot g^{-1}$ determined by porosimetry (corresponding to meso and macropores), an ash content of 2.6% (w/w), an iodine number of 1000 and the mercury and helium densities are 0.666 and 2.11 $g \cdot cm^{-3}$, respectively. The activated carbon was purified by Soxhlet extraction with HCl 2 $mol \cdot dm^{-3}$ for 6 hours, washed with deionised water until pH 6−7 and then dried in an oven at 150 °C for 13 hours, under vacuum (carbon A1).

All reagents and solvents used in the modification of the activated carbon and in the anchoring of the copper(II) complex were purified by distillation, except for copper(II) acetylacetonate, which was used as received. Copper(II) acetylacetonate and bis(3-aminopropyl)-amine (*trien*) were from Aldrich, and thionyl chloride, toluene and all other chemicals were from Merck (pro analysi).

$[Cu(acac)_2]$, XPS spectrum (eV): C 1s, 285.0 and 287.2; O 1s, 532.0; Cu $2p_{3/2}$, 934.8.

Functionalisation of Activated Carbon

Oxidation of Activated Carbon: The purified NORIT ROX 0.8 activated carbon (carbon A1; 22.0 g) was refluxed with a 5 mol·dm^{-3} solution of nitric acid (600 cm^3) for 7 hours. The oxidised carbon was extensively washed with deionised water until pH 6−7 and then dried in an oven at 150 °C for 13 hours, under vacuum (carbon A2).[18,23]

Reaction with Thionyl Chloride ($SOCl_2$): The oxidised activated carbon (12.0 g) was refluxed with 40 cm^3 of a 5% (v/v) solution of thionyl chloride in toluene for 5 hours, extensively washed with toluene, and then purified by Soxhlet extraction with toluene for 2 hours, and finally dried in an oven at 150 °C for 13 hours, under vacuum (carbon A3).[23,38]

Functionalisation with Bis(3-aminopropyl)amine (Trien): Carbon A3 (3.0 g) was refluxed with a solution containing 390 μmol of bis(3-aminopropyl)amine (*trien*) in 40 cm^3 toluene for 4 hours, then filtered and extensively washed with toluene. The material was also Soxhlet extracted for 2 hours with toluene and dried in an oven at 150 °C for 13 hours, under vacuum (carbon A4).

Anchoring of [Cu(acac)$_2$] onto the A4 Carbon: The activated carbon functionalised with *trien* (A4, 2.0 g) was added to 100 cm^3 of a solution of [Cu(acac)$_2$] in toluene (290 μmol), and the mixture was refluxed for 5 hours; during the reflux a progressive disappearance of the solution colour was observed. The resulting material was extensively washed with toluene and then purified by Soxhlet extraction with toluene for 7 hours, and dried in an oven at 150 °C for 13 hours, under vacuum (carbon A5).

Anchoring of [Cu(acac)$_2$] onto the A2 Carbon: The oxidised activated carbon A2 (2.0 g) was added to 100 cm^3 of a solution of [Cu(acac)$_2$] in toluene (335 μmol), and the mixture was refluxed for 5 hours, and a progressive disappearance of the solution colour was also observed. The resulting material, carbon A6, was extensively washed with toluene and then purified by Soxhlet extraction with toluene for 7 hours, and dried in an oven at 150 °C for 13 hours, under vacuum (carbon A6).

Anchoring of [Cu(acac)$_2$] onto the A3 Carbon: The activated carbon functionalised with acyl chloride groups (A3, 2.0 g) was added to 100 cm^3 of a solution of [Cu(acac)$_2$] in toluene (229 μmol), the mixture was refluxed for 5 hours, and a progressive disappearance of the solution colour was observed. The resulting material was extensively washed with toluene and then purified by Soxhlet extraction with toluene for 7 hours, and dried in an oven at 150 °C for 13 hours, under vacuum (carbon A7).

Physico-Chemical Measurements

X-ray photoelectron spectroscopy was carried out at "Centro de Materiais da Universidade do Porto" (Portugal), in a VG Scientific ESCALAB 200A spectrometer using a non-monochromatized Mg-*Kα* radiation (1253.6 eV). The metal complex was compressed into a pellet prior to the XPS study. In order to correct for possible deviations caused by electric charge on the samples, the C 1s line at 284.6 eV was taken as internal standard.[39,40]

The textural characterisation of carbon-based materials was based on the N_2 adsorption isotherms, which were determined at 77 K with a Coulter Omnisorp 100 CX apparatus. The samples were degassed at 350 °C (A1) or at 120 °C (all other samples) until a final vacuum of 10^{-6} Torr was reached. The volume (V_{micro}) and mesopore surface area (S_{me}) were determined by the *t*-method, using the standard isotherm for carbon materials proposed by Reinoso et al.[41] The pore volume at $p/p_0 = 0.95$ ($V_{0.95}$) was estimated from the N_2 uptake (using the value of 0.8081 as the density of N_2 in its normal liquid state); the porosity volume, other than that due to the micropores (which accounts for most of mesopores − V_{me}), was calculated by subtracting the micropore volume, (V_{micro}), obtained by the *t*-method at $p/p_0 = 0.95$, ($V_{0.95}$), from the pore volume.[42]

Elemental analysis of C, H, and N were performed with a Carlo−Erba EA 1108 Elemental Analyzer. Metal analysis was performed by Kingston Analytical Services, U.K.

The thermograms were recorded with a Mettler TA 4000 thermal analyser, using a heating rate of 5 K·min^{-1} and a flow rate of the N_2 carrier gas of 200 cm^3·min^{-1}. The TPD profiles were obtained with a custom built set-up, consisting of a U-shaped tubular microreactor, placed inside an electrical furnace. The flow rate of the helium carrier gas (25 cm^3·min^{-1}) and the heating rate of the furnace (5 K·min^{-1}) were controlled with appropriate units. The masses at $m/z = 28$ and 44 were monitored with a Spectramass Dataquad quadrupole mass spectrometer.

EPR spectra of powdered samples diluted in KBr (5%) were obtained with an X band Bruker ESP 300 E spectrometer, at room temperature and at 120 K. The spectra were calibrated with diphenylpicrylhydrazyl (dpph) with $g = 2.0037$, and the magnetic field was calibrated using Mn^{II} in MgO. Typical experimental conditions were − modulation frequency: 100 kHz; modulation amplitude: 9 G; microwave power: 5 mW. The EPR parameters were obtained by simulation using the program Win EPR Simfonia (Bruker) assuming axial or rhombic Spin Hamiltonians. The reported values of $g_\perp$ (or g_x and g_y) and $A_\perp$ (or A_x and A_y) are less accurate because of their dependence on the used line widths (20−60 G).

Acknowledgments

The authors are indebted to Dr. Carlos Sá (CEMUP) for assistance with XPS analysis and to NORIT N.V., Amersfoort, Netherlands, for providing the activated carbon. A. R. S. thanks "Fundação para a Ciência e Tecnologia" (Lisboa) and the European Social Fund for a fellowship.

[1] D. A. Evans, M. M. Faul, M. T. Bilodeau, *J. Org. Chem.* **1991**, *56*, 6744−6746.
[2] Z. Li, K. R. Conser, E. N. Jacobsen, *J. Am. Chem. Soc.* **1993**, *115*, 5326−5327.
[3] C.-M. Che, H.-L. Kwong, W.-C. Chu, K.-F. Cheng, W.-S. Lee, H.-S. Yu, C.-T. Yeung, K.-K. Cheung, *Eur. J. Inorg. Chem.* **2002**, 1456−1463.
[4] S. Bunce, R. J. Cross, L. J. Farrugia, S. Kunchandy, L. L. Meason, K. W. Muir, M. O′Donnell, R. D. Peacock, D. Stirling, S. J. Teat, *Polyhedron* **1998**, *17*, 4179−4187.
[5] C. R. Jacob, S. P. Varkey, P. Ratnasamy, *Microporous Mesoporous Mater.* **1998**, *22*, 465−474.
[6] L. Canali, D. C. Sherrington, *Chem. Soc. Rev.* **1999**, *28*, 85−93.
[7] Q.-H. Fan, Y.-M. Li, A. S. C. Chan, *Chem. Rev.* **2002**, *102*, 3385−3466.
[8] N. E. Leadbeater, M. Marco, *Chem. Rev.* **2002**, *102*, 3217−3274.
[9] C. E. Song, S. Lee, *Chem. Rev.* **2002**, *102*, 3495−3524.
[10] D. Brunel, N. Belloq, P. Sutra, A. Cauvel, M. Laspéras, P. Moreau, F. Di Renzo, A. Galarneau, F. Fajula, *Coord. Chem. Rev.* **1998**, *178−180*, 1085−1108.
[11] J. S. Rafelt, J. H. Clark, *Catal. Today* **2000**, *57*, 33−44.
[12] I. W. C. E. Arends, R. A. Sheldon, *Appl. Catal. A* **2001**, *212*, 175−187.

[13] F. Rodríguez-Reinoso, *Carbon* **1998**, *36*, 159−175.
[14] A. J. Bird, in: *Catalyst Supports and Supported Catalysts* (Ed. A. B. Stiles), Butterworths, Boston, **1987**, chapter 5.
[15] P. C. L′Argentière, E. A. Cagnola, D. A. Liprandi, M. C. Román-Martínez, C. Salinas-Martínez de Lecea, *Appl. Catal. A* **1998**, *172*, 41−48.
[16] J. A. Díaz-Auñón, M. C. Román-Martínez, C. Salinas-Martínez de Lecea, P. C. L′Argentière, E. A. Cagnola, D. A. Liprandi, M. E. Quiroga, *J. Mol. Catal. A: Chem.* **2000**, *153*, 243−256.
[17] J. A. Díaz-Auñón, M. C. Román-Martínez, C. Salinas-Martínez de Lecea, *J. Mol. Catal. A* **2001**, *170*, 81−93.
[18] J. L. Figueiredo, M. F. R. Pereira, M. M. A. Freitas, J. J. M. Órfão, *Carbon* **1999**, *37*, 1379−1389.
[19] R. C. Sosa, R. F. Parton, P. E. Neys, O. Lardinois, P. A. Jacobs, P. G. Rouxhet, *J. Mol. Catal. A* **1996**, *110*, 141−151.
[20] R. F. Parton, P. E. Neys, P. A. Jacobs, R. C. Sosa, P. G. Rouxhet, *J. Catal.* **1996**, *164*, 341−346.
[21] A. Valente, A. M. Botelho do Rego, M. J. Reis, I. F. Silva, A. M. Ramos, J. Vital, *Appl. Catal. A* **2001**, *207*, 221−228.
[22] A. R. Silva, C. Freire, B. de Castro, M. M. A. Freitas, J. L. Figueiredo, *Microporous Mesoporous Mater.* **2001**, *46*, 211−221.
[23] A. R. Silva, M. Martins, M. M. A. Freitas, A. Valente, C. Freire, B. de Castro, J. L. Figueiredo, *Microporous Mesoporous Mater.* **2002**, *55*, 275−284.
[24] A. R. Silva, C. Freire, B. de Castro, M. M. A. Freitas, J. L. Figueiredo, *Langmuir* **2002**, *18*, 8017−8024.
[25] A. R. Silva, J. Vital, J. L. Figueiredo, C. Freire, B. de Castro, *New J. Chem.* **2003**, *27*, 1511−1517.
[26] A. R. Silva, J. L. Figueiredo, C. Freire, B. de Castro, *Microporous Mesoporous Mater.*, **2004**, *68*, 83−89.
[27] A. R. Silva, C. Freire, B. de Castro, *New J. Chem.*, **2004**, *28*, 253−260.
[28] I. N. Neves, C. Freire, A. N. Zakhárov, B. de Castro, J. L. Figueiredo, *Colloids Surf. A. Physicochem. Eng. Aspects* **1996**, *115*, 249−256.
[29] R. Ferreira, M. Silva, C. Freire, B. de Castro, J. L. Figueiredo, *Microporous Mesoporous Mater.* **2000**, *38*, 391−401.
[30] R. Ferreira, C. Freire, B. de Castro, A. P. Carvalho, J. Pires, M. Brotas de Carvalho, *Eur. J. Inorg. Chem.* **2002**, 3032−3038.
[31] J. Pires, J. Francisco, A. P. Carvalho, M. Brotas de Carvalho, A. R. Silva, C. Freire, B. de Castro, *Langmuir*, in press.
[32] A. P. Carvalho, C. Castanheira, B. Cardoso, J. Pires, A. R. Silva, C. Freire, B. de Castro, M. Brotas de Carvalho, *J. Mater. Chem.*, **2004**, *14*, 374−379.
[33] R. J. J. Janssen, H. van Bekkum, *Carbon* **1995**, *33*, 1021−1027.
[34] A. H. Maki, B. R. McGarvey, *J. Chem. Phys.* **1958**, *29*, 31−34.
[35] H. R. Gersmann, J. D. Swalen, *J. Chem. Phys.* **1962**, *36*, 3221−3233.
[36] J. I. Zink, R. S. Drago, *J. Am. Chem. Soc.* **1972**, *94*, 4550−4554.
[37] H. Yokoi, A. W. Addison, *Inorg. Chem.* **1977**, *16*, 1341−1349.
[38] J. C. Lennox, R. W. Murray, *J. Electroanal. Chem.* **1977**, *78*, 395−401.
[39] J. F. Moulder, W. F. Stickle, P. E. Sobol, K. D. Bomben, in: *Handbook of X-ray Photoelectron Spectroscopy* (Ed. J. Chastain), Perkin−Elmer, **1992**.
[40] Y. M. Xie, P. M. A. Sherwood, *Chem. Mater.* **1990**, *2*, 293−299.
[41] F. Rodríguez-Reinoso, J. M. Martin-Martinez, C. Prado-Burguet, B. McEnaney, *J. Phys. Chem.* **1987**, *91*, 515−516.
[42] Z. Hu, M. P. Srinivasan, *Microporous Mesoporous Mater.* **2001**, *43*, 267−275.

Received October 29, 2003
Early View Article
Published Online April 1, 2004

